

Near-threshold continuum structure and the dissociation energies of H₂, HD, and D₂

E. E. Eyler and N. Melikechi

Department of Physics and Astronomy, University of Delaware, Newark, Delaware 19716

(Received 8 April 1993)

Using laser double-resonance spectroscopy, we have studied the second dissociation limit of all three stable isotopic variants of molecular hydrogen. Just above threshold, the vibrational continuum exhibits considerable fine-grained structure, differing greatly between isotopes because of varying nonadiabatic couplings between the B , B' , and C states. Significantly improved values of the dissociation energies are obtained from the continuum onsets. We also report preliminary investigations of atomic $2S:2P$ branching ratios very near threshold.

PACS number(s): 35.20.Gs, 33.80.Gj, 33.80.Rv

The second dissociation limit of H₂, converging to H(1S)+H(2P or 2S), is surprisingly complex because the $n=2$ atom can be in any of the closely spaced $2S_{1/2}$, $2P_{1/2}$, or $2P_{3/2}$ states. Thus careful investigation of the threshold region can yield not only improved values for the dissociation energy, but also a wealth of information on the energy-level structure and perturbations of long-range molecular states.

After Herzberg's high-resolution spectroscopic study of this region in 1970 [1] there was little experimental activity for many years. This hiatus has recently been ended by the development of efficient methods for producing tunable far-uv laser radiation with very narrow bandwidths. Direct single-photon spectroscopy in the extreme uv region has been used by Balakrishnan and Stoicheff to measure the dissociation energies of H₂ and D₂ by observing the onset of H(2S_{1/2}) atom production, with a resolution of about 0.25 cm⁻¹ [2,3]. McCormack and Eyler used double-resonance methods to observe the uppermost bound levels of H₂ with even higher resolution, about 0.01–0.02 cm⁻¹ [4]. We describe the extension of this work to include the near-threshold continuum in all three stable isotopic variants of molecular hydrogen. The resolution of ≤ 0.02 cm⁻¹ is much higher than for any previous studies of molecular dissociation continua. This paper reports results on near-threshold structure, atomic $2S:2P$ branching ratios, and improved determinations of the dissociation limits. Further experimental details are provided in a forthcoming publication that will also describe bound-state energy levels and quasibound resonances above the dissociation limit [5].

Optical double resonance through the $EF^1\Sigma_g^+$ state offers two advantages over direct vacuum uv excitation: state selectivity and a considerably reduced Doppler width. The drawbacks are increased complexity and excess noise caused by the need to spatially and temporally overlap multiple pulsed lasers that excite a highly nonlinear process. In the experiments reported here, this noise was exacerbated by a pump laser that operated on a small number of longitudinal cavity modes, jumping erratically between them.

The choice of which vibrational level in the EF state is used for the intermediate resonance does not greatly

affect the observed spectra, though it is obviously advantageous to select a level spanning a wide range of internuclear separations, to improve the vibrational overlap with near-threshold levels. We used the $v=6$, $N=0, 1$, and 2 levels in H₂, the $v=9$, $N=0, 1$, and 2 levels in D₂, and the $v=6$, $N=0$ and 1 levels in HD.

While transitions to the vibrational continua of all three of the $B^1\Sigma_u^+$, $C^1\Pi_u$, and $B'^1\Sigma_u^+$ states are possible, the C state potential has a barrier about 100 cm⁻¹ high that prevents direct dissociation, and the $B^1\Sigma_u^+$ has essentially no adiabatic amplitude because of very small vibrational overlap factors [6]. If the adiabatic approximation were to hold rigorously, near-threshold dissociation would occur only through the B' potential, which converges to H(1S)+H(2S). The shape of the near-threshold continuum should then be well-described by the Wigner threshold law [7],

$$\sigma = E^{N+1/2}. \quad (1)$$

Thus spectra obtained from $N=0$, in which only the $N=1$ continuum can be excited, should exhibit a $\frac{3}{2}$ -power law. The $N=1$ spectra can include both $N=0$ and $N=2$ continua, but $N=0$ should dominate very near threshold, because its square-root threshold law rises much faster. This idealized behavior can be altered by shape resonances, nonadiabatic couplings between the B , B' , and C states, and perturbations due to fine and hyperfine interactions. It is at best a very rough approximation.

The experiment uses the arrangement described in Ref. [4], except that a variety of different detection methods have been used to disentangle the near-threshold structure and to allow selective detection of atomic 2(S) or 2(P) dissociation products. In each of these methods, atomic or molecular ions are produced either by resonant or nonresonant multiphoton ionization (MPI). To separate ionic species by their time of flight we conduct the measurements in static dc electric fields of 50–200 V/cm. Field-induced energy shifts should be negligibly small, since the polarizabilities of near-threshold levels should be similar to those of H($n=2$) atoms. For several runs the field was varied to ascertain that there is no measurable effect apart from the expected shortening of

the $H(2S_{1/2})$ lifetime by mixing with $H(2P_{1/2})$.

Altogether five different detection schemes have been used, although not all were practical for all eight thresholds. The first two schemes are the same ones described in Ref. [4], in which multiphoton ionization by the same red laser used to excite the threshold region produces either H_2^+ or H^+ ions. As a general rule, the H_2^+ detection channel is sensitive primarily to bound states and the H^+ channel to the continuum, although we have found several bound levels that behave oppositely. In the third detection scheme, a delayed pulse from a third laser tuned to the atomic Balmer- α transition is used to selectively detect metastable H or D atoms by resonant MPI. The fourth scheme is a variation in which the Balmer- α laser is simultaneous with the probe laser, detecting both $2S$ and $2P$ atoms. The final detection scheme is depletion spectroscopy, measuring total photoabsorption from the EF state. To accomplish this the third laser is delayed by about 40 nsec and tuned off-resonance, and its power is increased to produce nonresonant MPI of the EF state. The resulting ion signal is reduced whenever molecules are excited by the probe laser, since it depletes the EF state population.

Figures 1–4 depict threshold scans from $N=1$ for all three isotopic variants. The other threshold scans will be presented in Ref. [5]. All five detection methods are shown for H_2 , for which the continuum amplitude is largest. Direct detection of $2S$ or $2P$ atoms is in principle the most informative method, but excessively high laser powers at the Balmer- α transition were needed to obtain sufficient signals, causing spurious signals due to bound states as well as broadening of the $2S+2P$ spectra. Therefore MPI detection, though less selective, was generally more useful. Depletion spectroscopy has so far been practical only for the $N=1$ threshold in H_2 . It closely matches the H^+ MPI scan, indicating that the MPI spectra correspond well to the total photoabsorption cross sections.

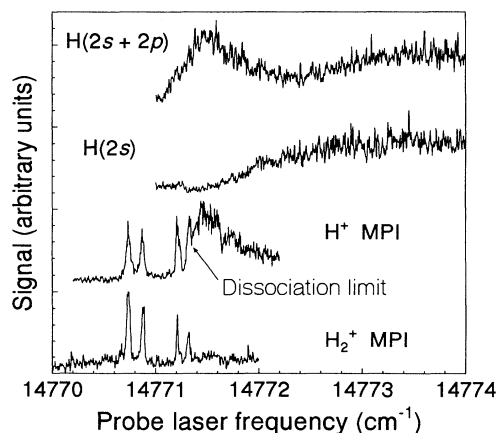


FIG. 1. Threshold scans from EF , $v=6$, $N=1$ in H_2 showing various detection channels. The apparent $2P$ atom signal slightly below threshold is caused by the power broadening of the $2P$ state by the Balmer- α detection laser.

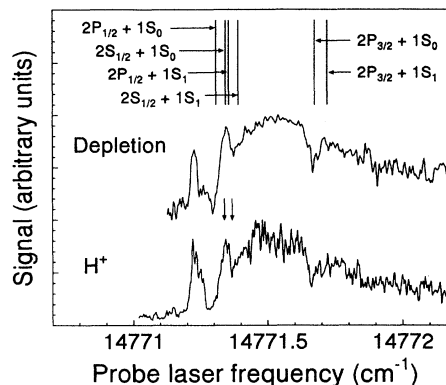


FIG. 2. Comparison of H^+ and depletion scans in the immediate vicinity of the $N=1$ threshold of H_2 . Vertical arrows are upper and lower limits for threshold (see text). Theoretical dissociation limits from Ref. [16] are also shown, including atomic $n=2$ fine structure and $n=1$ hyperfine structure.

In most cases the $2S$ and $2S+2P$ scans are very similar in appearance, showing that the near-threshold continuum consists principally of metastable $2S_{1/2}$ atoms. This is consistent with the expectation that the B' state carries most of the near-threshold oscillator strength. However, Glass-Maujean, Frohlich, and Beswick have shown that nonadiabatic effects can alter this situation, at least further above threshold [8].

Thus it is not too surprising that we find an exception for the $N=1$ threshold in H_2 , shown in Fig. 1. Here an extremely sharp threshold is observed in MPI, immediately after the highest bound resonance. The absence of a $H(2S)$ signal in the first 0.25 cm^{-1} shows that dissociation occurs entirely to $2P_{1/2}$ atoms, and the very sharp edge suggests that the dissociation involves the B state, whose slowly rising C_3/R^3 long-range potential curve would produce an abrupt continuum onset. It is likely that this behavior is indirectly attributable to a strong resonance with the quasibound $v=13$, $N=2$ level of

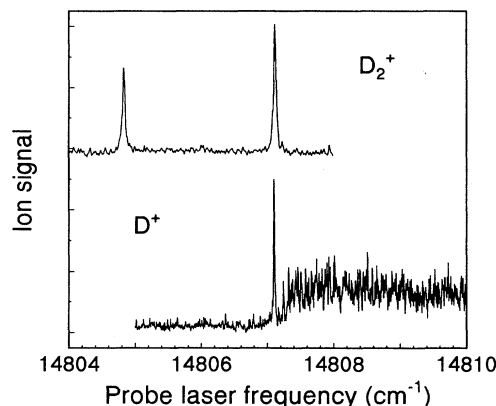


FIG. 3. Threshold region in D_2 , from $N=1$ of EF , $v=9$. Balmer- α detection was not practical because of artifacts caused by the strong resonance just below threshold.

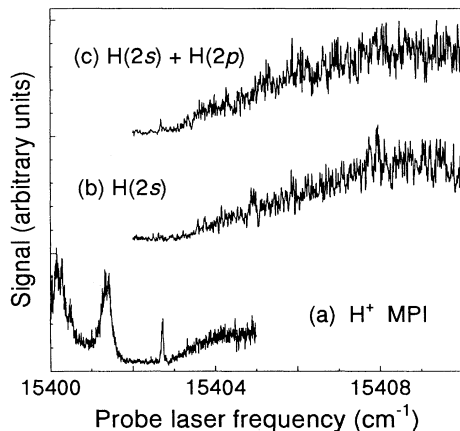


FIG. 4. Threshold region in HD, from $N=1$ of EF , $v=6$.

$C^1\Pi_u^+$, for which calculations predict appreciable non-adiabatic mixing with the B state [9]. This could also account for surprisingly strong transitions observed to bound B state levels just below threshold, which would be unobservably weak in the adiabatic approximation. The $N=0$ and $N=2$ thresholds in H_2 are less remarkable, although in both cases excessive noise prevented study with the same detail as for $N=1$.

In D_2 , the $N=0$ threshold was observed in D^+ MPI and in $D(2S)$ production. It shows a fairly unstructured rise extending over about 0.5 cm^{-1} . The $N=1$ threshold in D_2 is dominated by an extremely strong bound-state transition barely below threshold, which we tentatively identify as $B'1\Sigma_u^+$, $v=13$, $N=2$. In the D^+ MPI spectrum shown in Fig. 3, the continuum can be clearly observed starting just above this bound state. The $N=2$ threshold is too weak to be usable.

In HD the $N=0$ scans show a weak but definite continuum with little structure. The continuum onset for $N=1$, shown in Fig. 4, is particularly smooth and gradual. This is presumably because the broad resonant C_3/R^3 long-range potential of the B state, which gives rise to much of the structure in H_2 , cannot exist in HD because of the 22-cm^{-1} separation of the $H+D^*$ and H^*+D thresholds.

In seven cases it was practical to determine accurate dissociation limits, which are summarized in Table I. In three of these cases, the threshold is sufficiently clean to permit fits to the Wigner threshold law by a least-squares procedure. For $N=0$ in D_2 the $D(2S)$ signal was fit to a $\frac{3}{2}$ -power law. For $N=1$ in HD fits were possible both for the H^+ MPI signal at the $(1S)+H(2S)$ limit and the $D(2S+2P)$ signal at the $H(1S)+D(2S)$ limit. Since the statistical uncertainties were smaller than model-dependent effects, the uncertainties were estimated from differences between fits to the appropriate threshold laws and simple linear extrapolations.

In four other cases the MPI signal sizes are usable but the Wigner-law behavior is badly obscured by bound states just below the continuum edge or by structure in the continuum. For these cases we instead use a

TABLE I. Dissociation thresholds from the EF state and $v=0$, $N=0$ of the $X^1\Sigma_g^+$ ground state. Measurements from the EF state are from $v=6$ for H_2 and HD, and from $v=9$ for D_2 .

	From EF state	From X state, $v=0$, $N=0$
H_2 , $N=0$	14 817.36(6)	118 377.00(7)
H_2 , $N=1$	14 771.35(2)	118 376.98(4)
D_2 , $N=0$	14 833.05(5)	119 029.65(7)
D_2 , $N=1$	14 807.17(5)	119 029.67(7)
HD, $N=0$	15 444.00(25)	118 664.80(30)
HD, $N=1$	15 402.94(7)	118 664.84(10)
HD, $N=1$ ($H+D^*$)	15 425.40(20)	118 687.30(21)

semiempirical procedure to set upper and lower limits for the dissociation threshold. The lower limit is determined by the position of the highest bound level, and the upper limit by estimating the lowest frequency at which the continuum can be unambiguously observed. Figure 2 shows a particularly clear-cut example for the $N=1$ threshold in H_2 , where the sharp continuum onset makes a very accurate determination possible. This procedure assumes that the bound levels lie below the lowest observable threshold, and are not quasibound resonances converging to higher fine-structure thresholds. Otherwise the continuum edge could overlap the resonance, and could lie lower by as much as its linewidth. This assumption is quite reasonable, since predissociation and quantum interference would be expected to alter the line shapes of above-threshold resonances. We have never yet observed sharp and purely positive-going resonances imbedded in the continuum.

To obtain the total dissociation energies, it is necessary to add the EF state energies. For H_2 we use the term energies determined by McCormack [10]. The uncertainty of the $v=6$, $N=1$ level is 0.02 cm^{-1} , while the $N=0$ level is accurate only to 0.04 cm^{-1} . The other isotopic variants are more problematic. Only the $v=0$ levels are included in recent high-accuracy measurements [11,12], so the higher vibrational levels must be determined by combining these data with older measurements of intervals between excited states. For D_2 we use the energy levels tabulated by Freund, Schiavone, and Crosswhite [13], applying a correction of 0.14 cm^{-1} obtained by comparison with accurate $v=0$ levels from Ref. [12]. The resulting accuracy is at least 0.05 cm^{-1} . For HD, to establish a

TABLE II. Comparison of recent results for the dissociation energies of H_2 , D_2 , and HD. Column labeled Δ shows differences between this work and theory.

	This work	Other measurements	Theory (Ref. [16])	Δ
H_2	36 118.06(4)	36 118.11(8) ^a	36 118.049	0.01(4)
D_2	36 748.32(7)	36 748.38(7) ^b	36 748.345	-0.03(7)
HD	36 405.88(10)	36 406.2(4) ^c	36 405.763	0.12(10)

^aReference [2].

^bReference [3].

^cReference [1].

connection between the accurately known $v=0$ level and $v=6$, we use the spectroscopic intervals reported in 1936 by Dieke [14]. Using combination differences from these spectra, we determine energies of $103\,220.80(7)\text{ cm}^{-1}$ for $v=6$, $N=0$, and $103\,261.90(7)\text{ cm}^{-1}$ for $N=1$. The final column of Table I shows the resulting values for the second dissociation limits.

Table II lists the ground-state dissociation energies D_0 , obtained from the results in Table I by subtracting appropriate H and D atom $1S$ - $2S$ intervals [15]. We assume the dissociation is to $2S_{1/2}$ atoms, except for H_2 , $N=1$, where it is known to be to $2P_{1/2}$. This assumption is beyond doubt only for D_2 , $N=0$, but the results would change by less than half the listed uncertainties if $2P$ production were assumed instead. It is also not clear in which hyperfine level the ground-state atoms are produced. This contributes appreciably to the error budget only for H_2 , $N=1$, for which an uncertainty of half the hyperfine interval is added in quadrature. For H_2 and HD the $N=1$ results carry nearly all of the statistical

weight, while for D_2 a weighted average of the two determinations is used. The uncertainty is reduced very little by averaging; it comes largely from the overall uncertainty of the EF state energy levels. Table II also shows the newest theoretical values by Kołos and Rychlewski [16], and other recent experimental determinations. The agreement is good in all cases.

With a better detection scheme, $2S:2P$ branching ratios could be systematically measured and the results for D_0 much improved. We plan to use a laser at about 367 nm to selectively excite $2S$ or $2P$ atoms to Rydberg states with $n \approx 25$, subsequently ionized by a delayed pulsed electric field.

We thank Benjamin Catching for valuable assistance in conducting the measurements, and Boris Stoicheff and Ashok Balakrishnan for helpful discussions. This research was supported by the NSF, Grant No. PHY-9019524.

-
- [1] G. Herzberg, *J. Mol. Spectrosc.* **33**, 147 (1970).
 [2] A. Balakrishnan, V. Smith, and B. Stoicheff, *Phys. Rev. Lett.* **68**, 2149 (1992).
 [3] A. Balakrishnan and B. P. Stoicheff, *J. Mol. Spectrosc.* **156**, 517 (1992).
 [4] E. F. McCormack and E. E. Eyler, *Phys. Rev. Lett.* **66**, 1042 (1991).
 [5] E. E. Eyler, B. Catching, and N. Melikechi (unpublished).
 [6] C. W. Zucker and E. E. Eyler, *J. Chem. Phys.* **85**, 7180 (1986).
 [7] A. R. P. Rau, *Comments At. Mol. Phys.* **14**, 285 (1984).
 [8] M. Glass-Maujean, H. Frohlich, and J. A. Beswick, *Phys. Rev. Lett.* **61**, 157 (1988).
 [9] P. Senn, P. Quadrelli, and K. Dressler, *J. Chem. Phys.* **89**, 7401 (1988).
 [10] E. F. McCormack, PhD thesis, Yale University, 1989.
 [11] J. M. Gilligan and E. E. Eyler, *Phys. Rev. A* **46**, 3676 (1992).
 [12] D. Shiner, J. M. Gilligan, B. M. Cook, and W. Lichten, *Phys. Rev. A* **47**, 4042 (1993).
 [13] R. S. Freund, J. A. Schiavone, and H. M. Crosswhite, *J. Phys. Chem. Ref. Data* **14**, 235 (1985).
 [14] G. H. Dieke, *Phys. Rev.* **50**, 797 (1936).
 [15] G. W. Erickson, *J. Phys. Chem. Ref. Data* **6**, 831 (1977).
 [16] W. Kołos and J. Rychlewski (unpublished).